Lasers in Manufacturing Conference 2019

Modeling and experimental validation of single-pulse and multi-pulse picosecond laser beam ablation of cemented tungsten carbide

Juan Pablo Calderón Urbina[a*], Claus Emmelmann[a,b]

[a]*Institute of Laser and System Technologies, Hamburg University of Technology, Denickestr. 17, Hamburg, 21073, Germany*
[b]*Fraunhofer Research Institution for Additive Manufacturing Technologies IAPT, Am Schleusengraben 14, Hamburg, 21029, Germany*

Abstract

Ultra-short pulse laser beam processing of ultra-hard and compound materials represents a challenge in the determination of correct parameters and settings efficient ablation. Therefore, this paper presents an approach for the modeling and validation of the ablation process on cemented tungsten carbide to gain understanding of an effective application of the technology. The model is based on the identification of the ablation threshold of the material by heat transfer fundamentals, the adaptation of the Beer-Lambert law to a picosecond laser pulse and the development of a multi-pulse ablation model supported by relevant known theories (e.g., Chichkov et Al., 1996; Darif and Semmar, 2008; Jaeggi et Al., 2011) and using single-pulse mode and partition of pulses into bursts. Experimental ablation depth shows a corresponding behaviour to the model in the analysis of a single pulse and multi-pulse irradiation with single-pulse mode, and an interesting phenomenon, both accurate and unexpected, with the application of multi-pulse irradiation with burst-mode in two levels.

Keywords: Laser ablation; Picosecond; burst-mode; cemented tungsten carbide; Modeling

1. Introduction

The possibility to use ultra-short pulse lasers for processing ultra-hard materials has led to several investigations on the influence of process and beam characteristics in the last decade. Leading publications

* Corresponding author. Tel.: +49-401-766-029-612 Fax: +49-404-840-109-99.
E-mail address: juan.calderon@tuhh.de.

focused on the effects of laser beam ablation on cemented tungsten carbide properties (Tan et Al., 2010), the feasibility and capability of ultra-short pulse laser applications (Klimt, 2011; Fischer, 2012), the laser preparation of cutting tools (Konrad et Al., 2012), the generation of cutting edges (Dold et Al., 2013), the analytical investigation of the laser beam ablation of cemented tungsten carbide (Calderón Urbina et Al., 2013), the influence of pulse length and wavelength on ablation (Eberle and Wegener, 2014) and the control of geometries and dimensions of ultra-short laser beam structuring of grinding tools (Walter et Al., 2014). These publications have contributed to the fundamental understanding of the use of ultra-short pulses and picosecond lasers in the processing of ultra-hard materials. However, the processing of ultra-hard materials represents a continuous challenge due to the variety of possible materials. The continuous development of ultra-hard materials results in different compositions and grain sizes that affect laser processing parameters and settings, and results in time consuming, costly and detailed experimentations for optimized laser ablation process parameters.

The objective of this work is to model the ablation depth from the analysis of the process of laser beam ablation and based on the properties of the material and the characteristics of the laser system. The model is validated by experimental results. The goal of this study is to introduce an adaptable initial material investigation model for optimized ablation parameters. The analysis on cemented tungsten carbide (WC) represents a first attempt in this direction. The proposed model is based on the collection of material and laser system properties and characteristics, the identification of the threshold fluence F_{th} by the use of the heat transfer fundamentals, the adaptation of the Beer-Lambert law to a picosecond pulse to determine the Gaussian input power intensity P_I and the input average fluence F to model one single pulse and set the basis for the modeling of multi-pulse laser ablation with single-pulse and burst-mode (partition of a pulse into bursts).

2. Methodology

2.1. Theoretical background

A previous work of the authors (Calderón Urbina et Al.) presented an initial approach on modeling of ultra-short pulses in laser ablation. A theoretical background and analysis that complements the concept presented in this investigation is shown in this previous work, e.g., the penetration depth δ. Knowing the material properties and laser system characteristics the calculation of F_{th} for one single pulse is essential for the proposed ablation model. This is done by the use of the heat transfer fundamentals (Chichkov et Al., 1996; Willis and Xu, 2002; Darif and Semmar, 2008), which describes the required total power density $E_{\upsilon T}$ to evaporate the material from solid-state. This analysis demands the calculation of the required power density to rise the temperature of a volume of the material to the targeted phase $E_{\upsilon\,(temperature)}$, and also, to change the physical phase of that volume $E_{\upsilon\,(phase)}$. These calculations have to be done from solid-state to liquid-state and from liquid-state to vaporous-state. The following heat transfer fundamental expressions describe the temperature change and the phase change in equation (1) and (2), respectively:

$$E_{\upsilon\,(temperature)} = C_p \cdot \rho \cdot \frac{dT}{dt} \tag{1}$$

$$E_{\upsilon\,(phase)} = \frac{LH \cdot \rho}{t} \tag{2}$$

In (1), C_p represents the heat capacity of the material, ρ the density of the material, *dT* represents the change in temperature and *dt* the period of time in which the change in temperature is achieved. In (2), *LH* represents the corresponding latent heat of the material phase change.

After the identification of $E_{\upsilon T}$, the calculation of F_{th} is done by the application of equation (3), where τ_H is the length of the laser pulse:

$$F_{th} = E_{\upsilon T} \cdot \tau_H \cdot \delta \tag{3}$$

The determination of F_{th} defines the ablation limits and helps the model to distinguish ablated from non-ablated zones. The following step consists in the description of the energy that is irradiated from the laser, having a Gaussian behavior and according to the Beer-Lambert law (Darif and Semmar, 2008). Equation (4) describes the input power intensity P_I that is delivered from a Gaussian laser pulse, and where E_0 is the pulse energy, *t* represents a period of time of τ_H, τ_{Hm} equals the half of τ_H, and $\pi \cdot \omega_0^2$ describes the area of the laser spot:

$$P_I = \frac{E_0}{\pi \cdot \omega_0^2 \cdot \tau_H} e^{\frac{4(t-\tau_{Hm})^2}{\tau_{Hm}^2}} \tag{4}$$

The average input fluence *F* is calculated from the average of all P_I, which correspond to each *t* of τ_H, and the product of τ_H, as expressed in (5):

$$F = \tau_H \cdot \frac{\sum_{i=1}^{m} \frac{E_0}{\pi \cdot \omega_0^2 \cdot \tau_H} e^{\frac{4(t_i-\tau_{Hm})^2}{\tau_{Hm}^2}}}{1 + 2 + \cdots + m} \tag{5}$$

In pulsed laser systems the magnitude of *F* depends on the interaction of laser beam power P_L and pulse repetition rate *f*. These parameters dictate the amount of energy that every pulse contains. The behavior of a pulse through the material is described by (6) and is based on the Beer-Lambert law (Darif and Semmar, 2008). In the Beer-Lambert law states a Gaussian P_I corresponds to the laser pulse intensity through time *I(t),* *R* represents the reflectivity factor at a temperature *T* and *Gt(y,t)* is the heat source power density distribution in depth *y* and time *t*:

$$Gt(y,t) = I(t) \cdot (1 - R(T)) \frac{e^{\frac{-y}{\delta}}}{\delta} \tag{6}$$

The *Gt(y,t)* distribution allows the visualization of a single laser beam pulse penetrating into the material, as modeled for a picosecond pulse on cemented WC in (Calderón Urbina et Al., 2013) and the determination of the ablation depth of a pulse under different system parameters and settings. In the case of multiple pulse irradiation, there are three main aspect to consider. First, the number of pulses irradiating the same spot $N_{(n)}$ with single-pulse mode or burst-mode; second, the threshold fluence for a $N_{(n)}$, taking into account the incubation effect *S;* and third, the description of the ablation depth including: $N_{(n)}$, the input fluence $F_{(n)}$ for a

selected f, P_L, mode level n (single or bursts) and F_{th} for a $N_{(n)}$. Equation (7) describes $N_{(n)}$ from f, focal diameter d_w, n and scanner speed v_s:

$$N_{(n)} = \frac{f \cdot d_w}{v_s} \cdot n \tag{7}$$

The calculation of F_{th} is based on the determination of $F_{th(1)}$ from equation (3) and includes the influence of the incubation factor of the material after multi-pulse irradiation (Jee et Al., 1988; Mannion et Al., 2004; Jaeggi et Al., 2011), as shown in (8):

$$F_{th} = F_{th(1)} \cdot N_{(n)}^{S-1} \tag{8}$$

Finally, all the required elements for the modeling of multi-pulse laser beam ablation are found. The ablation depth of a material can be described by the application of equation (9), based on (Chichkov et Al., 1996; Jaeggi et Al., 2011) and adapted to multiple pulse irradiation.

$$Z_{abl} = N_{(n)} \cdot \delta \, ln\left(\frac{F_{(n)}}{F_{th}}\right) \tag{9}$$

2.2. Experimental set-up and procedure

The modeling and further experimental validation of the single-pulse and multi-pulse picosecond laser beam ablation of cemented WC is done by the use of the information from the laser system and material. The following table lists the specific parameters and settings of the used picosecond laser beam source system for the modeling of one single pulse ablation and multi-pulse ablation (mode, pulse repetition rate and scanner speed).

Table 1. Laser system parameters and settings

Parameters	Setting	Unit
Laser beam power P_L	50	W
Pulse length τ_H	10	ps
Beam radius ω_0	14	µm
Wavelength λ	1064	nm
Mode (single / burst) n	1, 5, 10	-
Pulse repetition rate f	500, 1000	kHz
Scanner speed v_s	0.5, 1, 2, 5	m/s

The analyzed material is a cemented tungsten carbide homogenously composed of cobalt Co and WC with 12% Co and 88% WC, respectively. The material has a grain size of 0.5 µm and it is shaped as a square blank sample typically used for cutting tools (dimensions: 13 mm x 13 mm x 5 mm, L x W x H). Table 2 presents the

properties of the material for this analysis based on (Riedel, 2000; Somiya, 2003; Harrison et Al., 2004; Schlottmann, 2005; Harrison et Al., 2006; AZO Materials, 2019).

Table 2. Material properties

Properties	Value	Unit
Thermal conductivity k	164	W m^{-1} K^{-1}
Specific heat (solid-state) $C_{p,s}$	210	J kg^{-1} K^{-1}
Specific heat (liquid-state) $C_{p,l}$	292	J kg^{-1} K^{-1}
Mass density (solid-state) ρ_s	15930	kg m^{-3}
Mass density (liquid-state) ρ_l	14500	kg m^{-3}
Melting point T_m	3143	K
Boiling point T_b	6273	K
Latent heat of fusion LH_f	400 000	J kg^{-1}
Latent heat of evaporation LH_e	4 020 000	J kg^{-1}
Absorption index κ	3.77 (from W)	-

The theoretical analysis of this investigation is validated by experimental results. The procedure for single pulse ablation consists in the irradiation of pulses separated among them by the lowest pulse repetition rate and a high scanner speed achieving a non-overlapping ablation and including the energy levels projected in the model. The procedure for multi-pulse ablation consists in the ablation of unidirectional lines of 1 mm and following the projected parameters and settings of the model. The ablation for both cases is done on the material at a focus position Z_f of 0 mm and at an incidence angle γ of 90°. The experimental results are analyzed by the use of a laser confocal microscope and using an average range of 200 measurement lines on the ablated area to determine their ablation depth Z_{abl}.

2.3. Model

The application of equations (1) and (2) for every phase change and with the information of tables 1 and 2 allows to determine the F_{th} for cemented WC from equation (3). This helps to identify the border of ablation of the material. Equation (4) determines the input power density P_l being irradiated from the source and presenting a Gaussian distribution, as characterized for the laser, in the selected period of time of τ_H. The authors presented a period t of 0.5 ps in (Calderon Urbina et Al., 2013). The average of all P_l for the periods completing τ_H is included in (6) to describe the development of the picosecond pulse in cemented WC in terms of power density in time and depth. Thus, the modeling of ablation depth for one single picosecond pulse under the energy considerations at different f is possible and presented in the following section. Multi-pulse ablation modeling requires the calculation of $N_{(n)}$, the adjustment of F_{th} to multiple pulses (incubation effect), and the results of (3) and (4).

Table 3. Outcome of the analysis of laser beam ablation of cemented WC

Properties / characteristics	Value	Unit
Absorption coefficient α	4.45 x 10^{7}	m^{-1}
Penetration depth δ	2.25 x 10^{-8}	m
Power density $E_{\upsilon T}$	874485 x 10^{21}	W m^{-3}
Threshold fluence F_{th}	0.1964	J cm^{-2}
Average input fluence *F*		
at *f* = 400 kHz	8.54	J cm^{-2}
at *f* = 500 kHz	6.83	J cm^{-2}
at *f* = 800 kHz	4.27	J cm^{-2}
at *f* = 1000 kHz	3.41	J cm^{-2}
Reflectivity *R* *	0.33	-
Incubation factor *S* *	0.75	-
* Experimentally measured and calculated		

The analysis of multi-pulse ablation has to define the average input fluence from the source according to the number of pulses on the same spot and its relationship to their pulse energy distribution as a function of *f* and P_L. Two levels of *f* have been used for this investigation to simplify the understanding of the analysis. Table 4 presents the average input fluences for single pulse and burst-mode in two levels, *n* = 5 bursts and *n* = 10 bursts. Thus, this information complements and adjusts equation (9) to the chosen number of pulses on the same spot and makes possible the calculation and modeling of Z_{abl}.

Table 4. Average input fluence for single-pulse and burst-mode in the multi-pulse analysis at a low and high value of *f*

Pulse repetition rate *f*	$F_{(n)}$, *n* = 1	$F_{(n)}$, *n* = 5	$F_{(n)}$, *n* = 10	Unit
500 kHz	6.83	1.36	0.68	J cm^{-2}
1000 kHz	3.41	6.83	0.34	J cm^{-2}

3. Results and discussion

The parameters and settings previously presented fulfilled the analytical approach to model the behavior of ablation depth. The following figures illustrate the results of both models: single picosecond pulse ablation (figure 1) and multi-pulse picosecond pulse ablation (figure 2). Moreover, the results of the second model include the use of single-pulse mode and the application of two levels of burst-mode. Following the modeling of laser beam ablation, an experimental validation of each model was done. The experimental results are also illustrated in figures 1 and figure 2 for comparison.

A single picosecond pulse was modeled under different pulse energies and based on the Beer-Lambert law and Gaussian-shape. The experimental results in figure 1 present a similar behavior to the model and are within the range of the standard error. The modeled pulse at a *f* = 800 kHz is the only result that does not match its corresponding validation and exceeds its error. Further analysis and experimentation are required.

As expected, the behavior of the model and validation shows a decreasing trend in the depth of the ablation when the pulse energy is reduced.

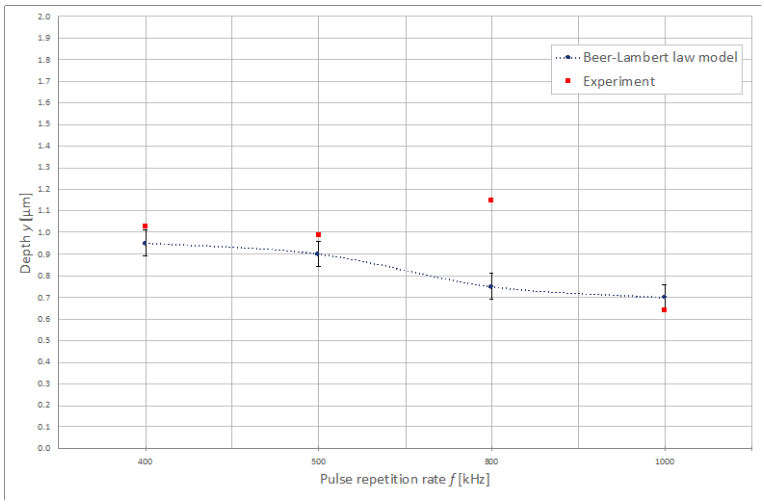

Fig. 1. Results of the model and experimental validation of a single picosecond pulse ablation on cemented WC

In the case of multi-pulse ablation with single-pulse mode, the validation experiments showed an ablation depth behavior outside of the error range at the lowest pulse repetition rate, see figure 2(a). On the other hand, at the highest pulse repetition rate the model presented more accurate results, as in figure 2(b). At lower pulse repetition rates, the pulse energy is high when compared to high repetition rates, and the experimental behavior of ablation depth is affected by other phenomena, e.g., plasma shielding; further analysis is required. The application of burst-mode presents accurate results (compared to the model) when v_s = 1 and 2 m/s for both n levels, see figure 2(c), 2(d), 2(e) and 2(f). However, with a n = 5 at the lowest and highest v_s, higher experimental values of ablation depth are obtained. In the case of n = 10 at a f = 500 kHz, a similar behavior to n = 5 is obtained. However, the results of n = 10 at a f = 1000 kHz present an unexpected result at the lowest v_s by the formation of a structure, as depicted in figure 2(f). This phenomenon could be originated due to the irradiation of a high number of pulses at low v_s. A similar behavior was already observed by the author at 800 kHz in other study. Further analysis is required.

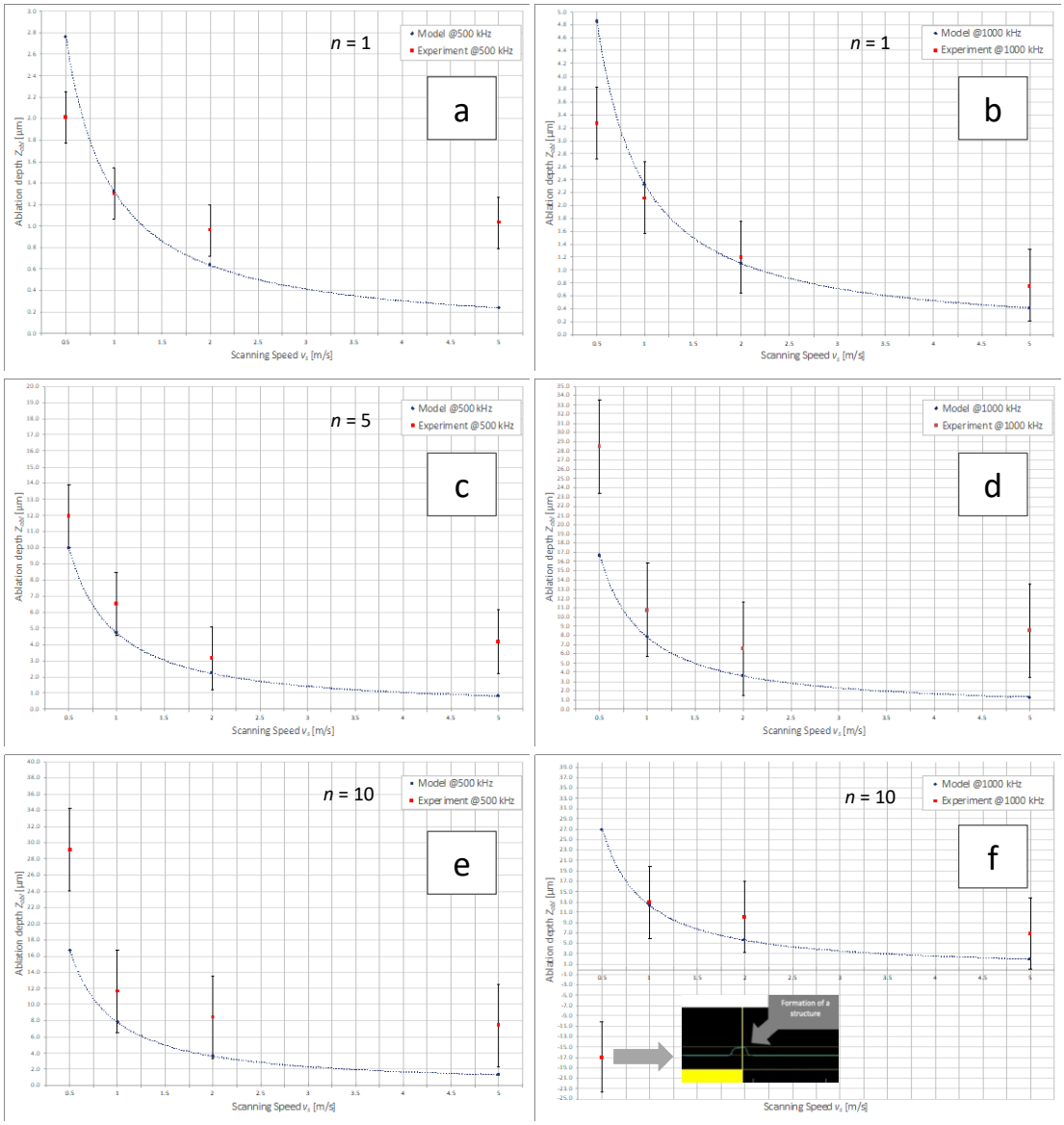

Fig. 2. Results of the model and experimental validation of multi-pulse picosecond ablation on cemented WC with single-pulse mode, at f = 500 kHz (a) and at f = 500 kHz (b); burst-mode n = 5, at f = 500 kHz (c) and at f = 500 kHz (d); and burst-mode n = 10, at f = 500 kHz (e) and at f = 500 kHz (f)

n = 5

4. Conclusion

A modeling of the ablation depth from the analysis of the process of laser beam ablation was presented. The models were based on the properties of the material and the characteristics of the system. A summary of the approach is illustrated in figure 3. The models included the analysis of the ablation of a single pulse, multiple pulses and burst-mode. The modeled results were validated by experiments. The results of the models and experiments were compared and gave both accurate and unexpected conclusions, e.g., a negative ablation depth. Further analysis of the experimental results will help calibrate the model and describe unexpected phenomena. High repetition pulse rates at a low scanner speed might avoid ablation due to excessive energy on the material. An analysis to define the borders of ablation with multiple pulses and burst-mode is required. In conclusion, this work introduced an initial adaptable material approach for the investigation of laser beam ablation on hard materials; moreover, knowledge was gained in the picosecond laser beam ablation of cemented WC.

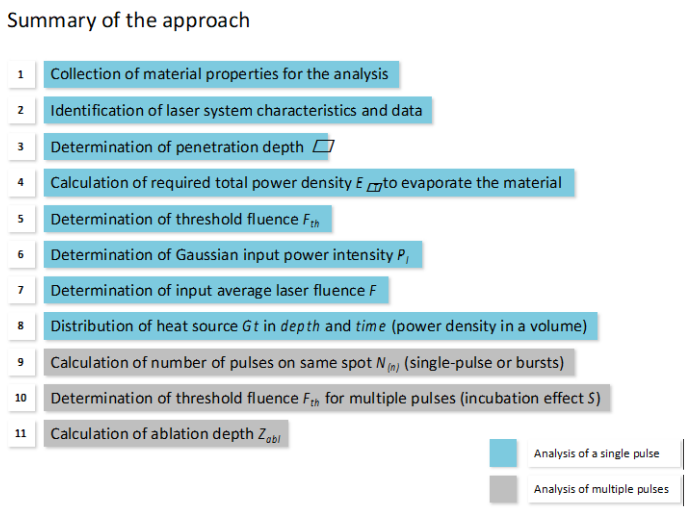

Fig. 3. Summary of the approach in this work

Acknowledgements

The presenting author would like to thank Dr. Dirk Herzog at the Hamburg University of Technology and the Fraunhofer Research Institution for Additive Manufacturing Technologies IAPT for the support on this publication.

References

Tan, J. L., Butler, D. L., Sim, L. M., Jarfors, A. E. W., 2010. "Effects of laser ablation on cemented tungsten carbide surface quality**",** Applied Physics A 101, p. 265 – 269.

Klimt, B., 2011. "Micromachining with ps-laser: Quality, Flexibility, Speed, Cost", Lumera Laser GmbH.

Fischer, T., 2012 "Grinding differend – Cutting tools manufacturing with picosecond laser", Light 2012. EWAG Körber AG, Hamburg.

Konrad, W., Dold, C., Marcel, H., Christian, W., 2012. "Laser prepared cutting tools", 7th International Conference on Photonic Technologies LANE 2012, Physics Procedia 39, p. 240 – 248.

Dold, C., Henerichs, M., Gilgen, P., Wegener, K., 2013. "Laser processing of coarse grain polycrystalline diamond (PCD) cutting tool inserts using picosecond laser pulses", Lasers in Manufacturing Conference 2013, Physics Procedia 41, p. 603 – 609.

Calderón Urbina, J. P., Christian, D., Emmelmann, C., 2013. "Experimental and analytical investigation of cemented tungsten carbide ultra-short pulse laser ablation", Lasers in Manufacturing Conference 2013, Physics Procedia 41, p. 752 – 758.

Eberle, G., Wegener, K., 2014. "Ablation study of WC and PCD composites using 10 picosecond and 1 nanosecond pulse durations at green and infrared wavelengths", 8th International Conference on Photonic Technologies LANE 2014, Physics Procedia 56, p. 951 – 962.

Walter, C., Komischke, T., Weingärtner, E., Wegener, K., 2014. "Structuring of CBN grinding tools by ultrashort pulse laser ablation", 6th CIRP International Conference on High Performance Cutting, HPC2014, Procedia CIRP 14, p. 31 – 36.

Chichkov, B. N., Momma, C., Nolte, S., von Alvensleben., Tünnermann, N., 1996. "Femtosecond, picosecond and nanosecond laser ablation of solids", Applied Physics A 63, p. 109 – 115.

Willis, D., A., Xu, X., 2002. "Heat transfer and phase change during picosecond laser ablation of nickel", International Journal of Heat and Mass Transfer 45, p. 3911 – 3918.

Darif, M., Semmar, N., 2008. "Numerical Simulation of Si Nanosecond Laser Annealing by COMSOL Multiphysics",In: COMSOL Conference 2008, COMSOL. Hannover.

Jee, Y., Becker, M.F., Walser, R.M., 1988. "Laser-induced damage on single-crystal metal surfaces", Journal of the Optical Society of America 5. Austin, U.S.A., p. 648-659.

Mannion, P. T., Magee, J., Coyne, E., O'Connor, G. M., Glynn, T. J., 2004. "The effect of damage accumulation behavior on ablation thresholds and damage morphology in ultrafast laser micro-machining of common metals in air", Applied Surface Science 233, p. 275 – 287.

Jaeggi, B., Neuenschwander, B., Schmid, M., Muralt, M., Zuercher, J., Hunziker, U., 2011. "Influence of the pulse duration in the ps-regime on the ablation efficiency of metals", Lasers in Manufacturing Conference 2011. Physics Procedia 12, p. 164 – 171.

Riedel, R., 2000. "Handbook of ceramic hard materials Part III Materials and applications", Wiley-VHC 2. Darmstadt, Weinheim.

Somiya, S., 2003. "Handbook of advanced ceramics", Elsevier.

Harrison, P. M., Henry, M., Henderson, I., Brownell, M. F., 2004. "Laser milling of metallic and nonmetallic substrates in the nanosecond regime with Q-switched diode pumped solid state lasers", Proceedings of SPIE, 5448, West Sussex, UK, p. 624-633.

Schlottmann, U., 2005. "SIDS Initial Assessment Report for SIAM 21 Tungsten Carbide", Bundesministerium fuer Umwelt, Naturschutz und Reaktorsicherheit, Washington D.C.

Harrison, P. M., Henry, M., Brownell, M. F., 2006. "Laser processing of polycristaline diamond, tungsten carbide and a related composite material", Journal of laser applications 18, West Sussex, UK, p. 177-187.

AZO Materials, 2019. Tungsten carbide – An overview, https://www.azom.com/properties.aspx?ArticleID=1203.